

1. Marine primary organic aerosol (MPOA) emission

The emission rate of MPOA is the product of sea spray aerosol (SSA) emission rate (E_{SSA}) and organic matter fraction of sea spray aerosol (OM_{SSA} , unitless in a range of 0~1), i.e.

$$E_{MPOA} = \alpha \times E_{SS} \times OM_{SS} \quad (1),$$

where OM_{SSA} is expressed as a function of wind speed, surface seawater Chl-a concentration, and aerosol size, and α is a tuning factor. The calculation of OM_{SSA} follows the method of Gantt et al. (2012):

$$OM_{SS} = \frac{\left(\frac{1}{1 + \exp(X(-2.63[Chl-a]) + X(0.18U_{10}))} \right)}{1 + 0.03 \exp(6.81D_p)} + \frac{0.03}{1 + \exp(X(-2.63[Chl-a]) + X(0.18U_{10}))} \quad (2),$$

where U_{10} is wind speed at 10 meter ($m\ s^{-1}$) simulated online by RIEMS-Chem, D_p is the diameter of sea salt aerosol, and Chl-a is the surface seawater chlorophyll-a concentration ($mg\ m^{-3}$). The Level-3 daily mean Chl-a concentration retrievals with 9 km resolution from the VIIRS onboard the SNPP satellite platform are used for model inputs and it can reflect day-to-day variation of sea surface Chl-a concentration associated with phytoplankton bloom in the western Pacific. X is a unitless adjustable coefficient and is set to 3 based on Gantt et al. (2012).

For the tuning factor α , Gantt et al. (2012) suggested a factor of 6 was able to minimize the relative model biases for the global model GEOS-Chem at two oceanic sites (Mace Head in North Atlantic and Amsterdam Island in remote south Indian Ocean). In this study, we found that a factor of 2 was optimal to obtain the least bias between model simulation and observation over the western Pacific.

2. Marine isoprene emission

The sea-air flux of marine isoprene (E_{isop} in the unit of $\mu g\ m^{-2}\ s^{-1}$) is parameterized following the method of Palmer and Shaw (2005), which can be expressed as:

$$E_{isop} = k \times SW_{isop} \quad (3),$$

where k is the sea-air exchange coefficient ($cm\ h^{-1}$) and is calculated as:

$$k = 0.31 \times U_{10} \times (660/Sc)^{1/2} \quad (4),$$

where Sc is the Schmit number of Isoprene.

The surface seawater isoprene concentration SW_{isop} ($\mu\text{g m}^{-3}$) related to phytoplankton activities is parameterized by the scheme of Gantt et al. (2009):

$$SW_{isop} = H_{\max} \times [Chl-a] \times \int_0^{H_{\max}} EF \ln(I)^2 dh \quad (5),$$

where EF is the emission factor of isoprene released by phytoplankton, I is the ambient photosynthetically active radiation (PAR, in the unit of $\mu\text{Em}^{-2} \text{s}^{-1}$), H_{\max} is the total water depth which isoprene production can occur from the surface to the point and is calculated as:

$$H_{\max} = -\ln\left(\frac{2.5}{I_0}\right) \frac{1}{k_{490}} \quad (6),$$

where I_0 is the all-sky surface incoming solar radiation (W m^{-2}) provided by the model during simulation. I_0 and I have an approximate relationship of $1 \text{ W m}^{-2} \approx 2 \mu\text{Em}^{-2} \text{s}^{-1}$. The diffuse attenuation coefficient values at 490 nm k_{490} (m^{-1}) is also obtained from VIIRS satellite. The isoprene production is assumed to occur when the light level is greater than 2.5 W m^{-2} in surface sea water.

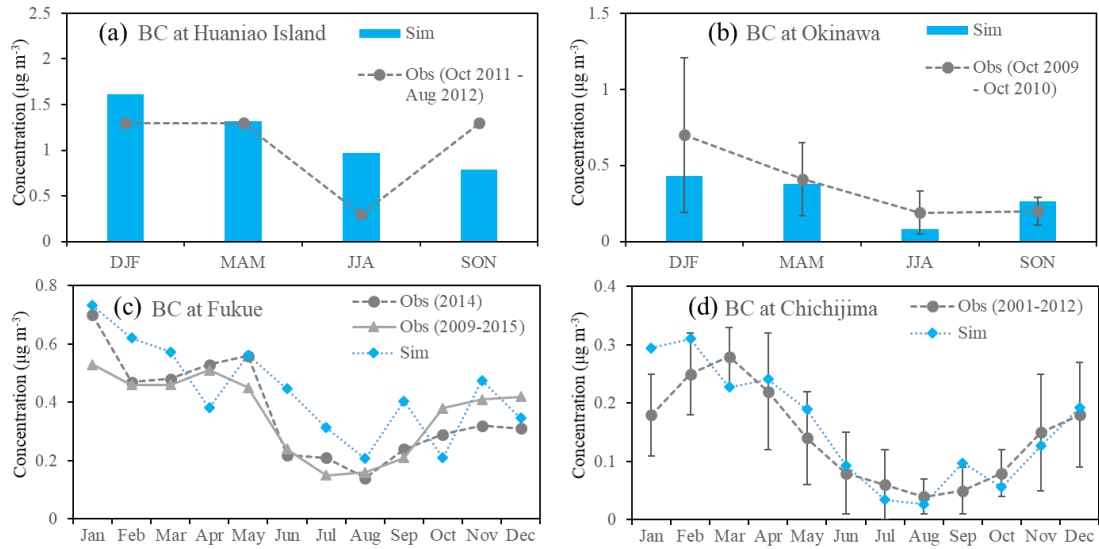


Figure S1. The model simulated (bars) and observed (dotted lines) BC concentrations at different sites. Seasonal mean concentrations were provided at (a) Huaniao Island (Wang et al., 2015) and (b) Okinawa (Kunwar and Kawamura, 2014) while monthly mean concentrations were provided at (c) Fukue (Kanaya et al., 2016) and (d) Chichijima Island (Boreddy et al., 2018). The observed sample standard deviations were available at Okinawa and Chichijima. The simulation is for the year 2014.

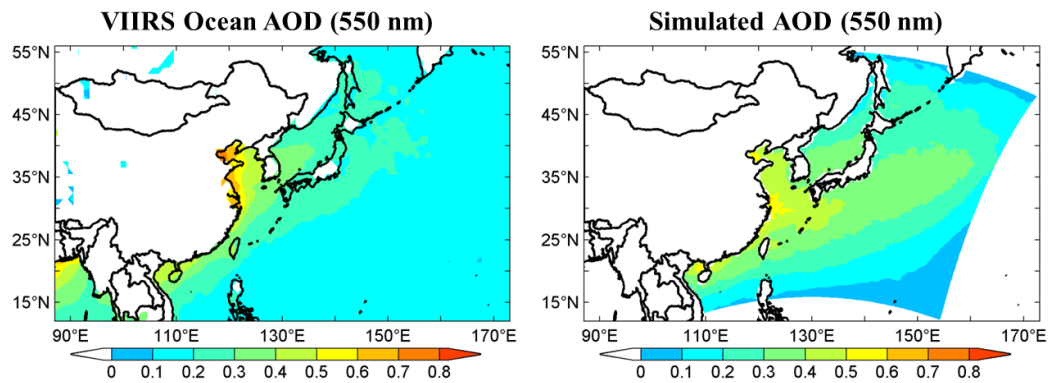


Figure S2. VIIRS retrieved (a) and model simulated (b) annual mean AOD at 550 nm over ocean. Values over the land have been masked. The model results were sampled accordingly to the satellite retrievals.

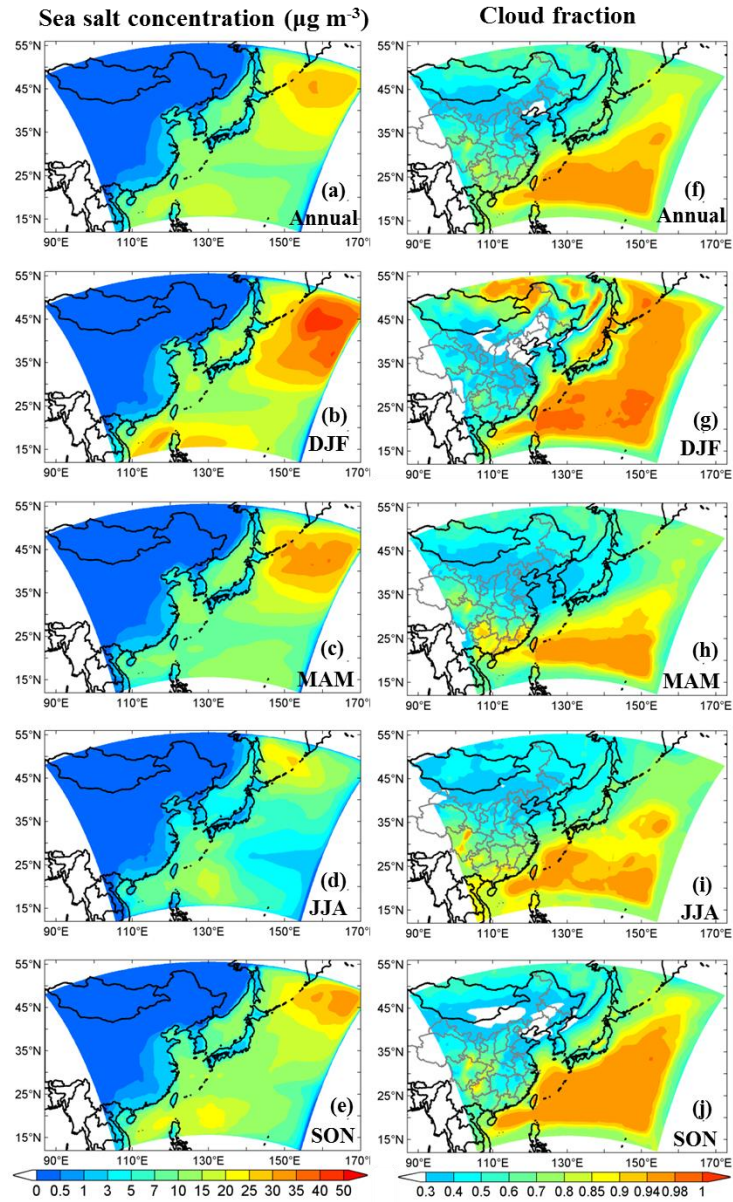


Figure S3. Model simulated annual and seasonal mean near surface sea salt concentrations (unit: $\mu\text{g m}^{-3}$) (a~e) and cloud fractions (unit: %) (f~j).

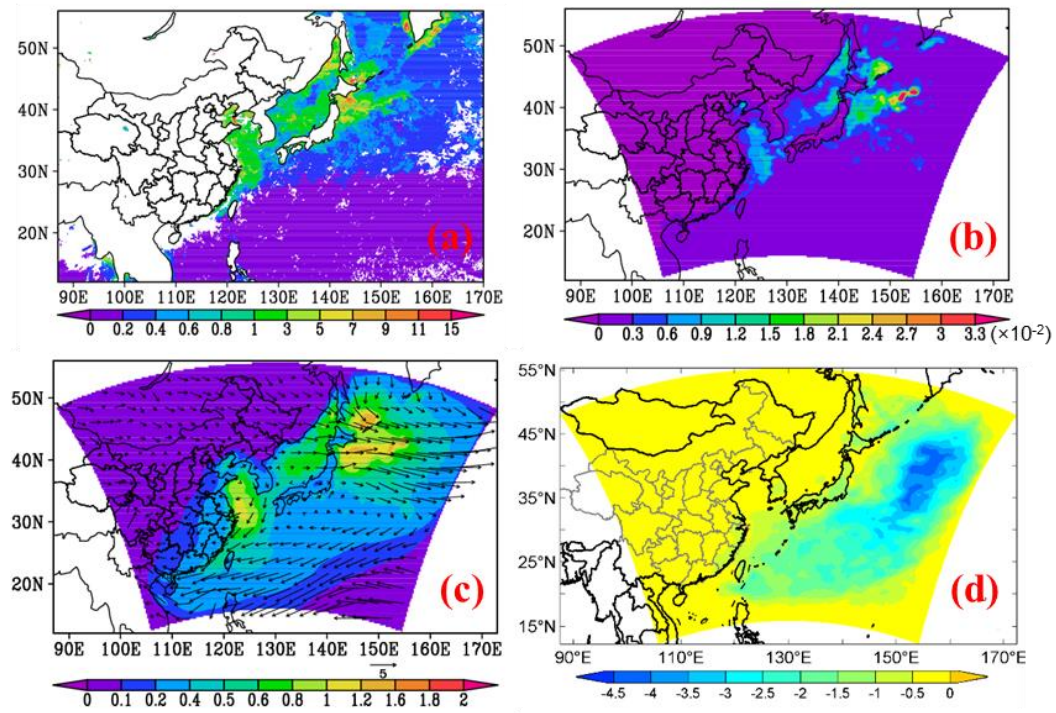


Figure S4. (a) VIIRS retrieved April mean Chl-a concentration (unit: mg m^{-3}), (b) model simulated April mean MPOA emission flux (unit: $\mu\text{g m}^{-2} \text{s}^{-1}$), (c) MOA concentration (unit: $\mu\text{g m}^{-3}$) overlaid with wind vector (unit: m s^{-1}), and (d) IRE_{MOA} (unit: W m^{-2}).

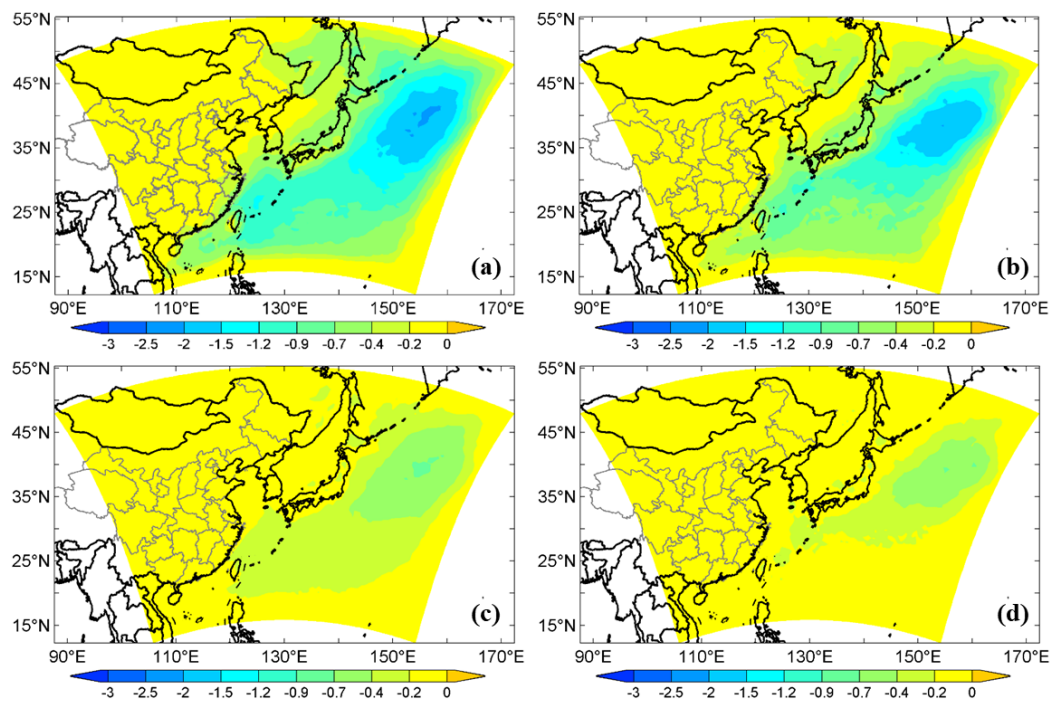


Figure S5. Annual mean IRE due to MOA from different sensitivity simulations. (a) FULL, (b) SENS1, (c) SENS2, and (d) SENS3.

Table S1. Observed (Obs) and simulated (Sim) annual mean sodium (Na^+) concentrations at EANET sites (units: $\mu\text{g m}^{-3}$). Pearson correlation coefficients (R) are presented.

Site	Samples	Obs	Sim	R
Rishiri	13	2.13	3.39	0.75
Tappi	22	2.89	1.84	0.78
Sado-seki	26	2.34	3.77	0.64
Oki	26	3.74	2.31	0.81
Hedo	24	4.79	2.89	0.53
Ogasawara	26	2.54	2.66	0.85
Total	137	3.14	2.78	0.50

Table S2. Performance statistics for hourly gas precursor concentrations (unit: pptv) at EANET sites for the year 2014. Mean observation (Obs), mean simulation (Sim), correlation coefficient (R), and normalized mean bias (NMB in %) are listed.

Sites	SO ₂				NO _x /NO ₂ ^a				O ₃						
	Samples	Obs	Sim	R	NMB	Samples	Obs	Sim	R	NMB	Samples	Obs	Sim	R	NMB
Rishiri	8493	0.22	0.21	0.62	-5	7606	0.70	0.96	0.27	38	8583	38.6	45.4	0.57	18
Tappi	8570	0.48	0.40	0.35	-15	8517	1.47	1.95	0.40	33	8569	39.3	48.0	0.52	22
Sado	8233	0.38	0.52	0.41	39	8200	0.75	2.91	0.39	286	8400	46.5	49.6	0.55	7
Oki	7837	0.54	0.45	0.54	-17	7919	1.32	1.66	0.39	26	8507	46.8	50.8	0.52	9
Hedo	7546	0.26	0.26	0.55	-2	7910	0.74	1.10	0.47	48	8260	39.6	41.5	0.84	5
Ogasawara	7635	0.10	0.11	0.09	5	7226	0.37	0.37	0.21	1	8506	33.4	35.8	0.84	7
Jeju	8282	0.54	0.76	0.41	42	8300	3.29	3.53	0.29	7	8419	44.7	52.5	0.56	17
Kanghwa	8517	2.77	4.09	0.25	48	8539	5.90	12.97	0.45	120	8526	50.3	29.4	0.55	-42
Imsil	8337	2.32	1.50	0.16	-35	8200	3.99	1.81	0.18	-55	8385	31.4	39.9	0.54	27
Average	73450	0.86	0.95	0.51	10	72417	2.12	2.87	0.48	36	76155	41.2	43.6	0.54	6

a: NO_x in Japan and NO₂ in Korea.

Table S3. Comparison of observational based estimated marine isoprene emission fluxes over different oceanic areas from previously published studies and model simulations (Units: $\text{nmol m}^{-2} \text{day}^{-1}$).

Locations ^a	Simulations from this study		Observations from previous studies		References
	periods	mean (max/min)	periods	mean (max/min)	
Western North Pacific (30.75~35.78°N, 146.42°E)	May 2014	85 (100/40)	18–26 May 2001	140 (300/32)	Matsunaga et al. (2002)
Northwest Pacific (34~43°N, 138~150°E)	Jan 2014 May 2014 Aug 2014	26.2 88.6 63.1	Jan 2008–2012 May 2008–2012 Aug 2008–2012	21.4 143.8 55.6	Ooki et al. (2015)
East China Sea (25.69~30°N, 121~126°E)	Oct–Nov 2013 May–Jun 2014	48 (120/0) 35 (180/0)	Oct–Nov 2013 May–Jun 2014	48.34 (169.15/4.19) 36.12 (137.75/2.46)	Li et al. (2018)
South Yellow Sea and East China Sea (30~38°N, 121.6~127°E)	Jul 2014	130 (240/0)	14 July – 1 Aug 2013	161.5 (537.2/22.17)	Li et al. (2017)
Southern Ocean ^b	Jul–Aug 2014	(400/0)	Dec 2010–Jan 2011	(313/181)	Kameyama et al. (2014)
Arctic Ocean ^b	Jul 2014	(400/0)	Jun–Jul 2010	(148/8.8)	Tran et al. (2013)

a: All the observations were conducted on research cruises and ranges of longitudes and latitudes indicate the coverages of each cruise.

b: Simulation results were restricted within the study domain of western North Pacific.

Table S4. Modeled domain and annual/seasonal mean IRE due to MOA from different sensitivity simulations.

	WP ^a	ECS ^b	NWP ^c
	ANN		
FULL	-0.66	-0.23	-1.04
SENS1	-0.53	-0.13	-0.81
SENS2	-0.20	-0.06	-0.34
SENS3	-0.14	-0.03	-0.24

a: Mean over oceanic areas.

b: 27~40°N, 115~123°E.

c: 35~55°N, 140~160°E.

Reference:

- Boreddy, S.K.R., Haque, M.M., and Kawamura, K.: Long-term (2001–2012) trends of carbonaceous aerosols from a remote island in the western North Pacific: an outflow region of Asian pollutants, *Atmos. Chem. Phys.*, 18, 1291–1306, <https://doi.org/10.5194/acp-18-1291-2018>, 2018.
- Gantt, B., Meskhidze, N., and Kamykowski, D.: A new physically-based quantification of marine isoprene and primary organic aerosol emissions, *Atmos. Chem. Phys.*, 9, 4915–4927, <https://doi.org/10.5194/acp-9-4915-2009>, 2009.
- Gantt, B., Johnson, M. S., Meskhidze, N., Sciare, J., Ovadnevaite, J., Ceburnis, D., and O'Dowd, C. D.: Model evaluation of marine primary organic aerosol emission schemes, *Atmos. Chem. Phys.*, 12, 8553–8566, <https://doi.org/10.5194/acp-12-8553-2012>, 2012.
- Kameyama, S., Yoshida, S., Tanimoto, H., Inomata, S., Suzuki, K., and Yoshikawa-Inoue, H.: High-resolution observations of dissolved isoprene in surface seawater in the Southern Ocean during austral summer 2010–2011, *J. Oceanogr.*, 70, 225–239, <https://doi.org/10.1007/s10872-014-0226-8>, 2014.
- Kanaya, Y., Pan, X., Miyakawa, T., Komazaki, Y., Taketani, F., Uno, I., and Kondo, Y.: Long-term observations of black carbon mass concentrations at Fukue Island, western Japan, during 2009–2015: constraining wet removal rates and emission strengths from East Asia, *Atmos. Chem. Phys.*, 16, 10689–10705, <https://doi.org/10.5194/acp-16-10689-2016>, 2016.
- Kunwar, B. and Kawamura, K.: One-year observations of carbonaceous and nitrogenous components and major ions in the aerosols from subtropical Okinawa Island, an outflow region of Asian dusts, *Atmos. Chem. Phys.*, 14, 1819–1836, <https://doi.org/10.5194/acp-14-1819-2014>, 2014.
- Li, J.-L., Zhang, H.-H., and Yang, G.-P.: Distribution and sea-to-air flux of isoprene in the East China Sea and the South Yellow Sea during summer, *Chemosphere*, 178, 291–300, 2017.
- Li, J.-L., Zhai, X., Zhang, H.-H., and Yang, G.-P.: Temporal variations in the distribution and sea-to-air flux of marine isoprene in the East China Sea, *Atmos.*

- Environ., 187, 131–143, 2018.
- Matsunaga, S., Mochida, M., Saito, T., and Kawamura, K.: In situ measurement of isoprene in the marine air and surface seawater from the western North Pacific, *Atmos. Environ.*, 36, 6051–6057, doi:10.1016/s1352-2310(02)00657-x, 2002.
- Ooki, A., Nomura, D., Nishino, S., Kikuchi, T., and Yokouchi, Y.: A global-scale map of isoprene and volatile organic iodine in surface seawater of the Arctic, Northwest Pacific, Indian, and Southern Oceans, *J. Geophys. Res.: Oceans* 120, 4108–4128, doi:10.1002/2014JC010519, 2015.
- Palmer, P. I. and Shaw, S. L.: Quantifying global marine isoprene fluxes using MODIS chlorophyll observations, *J. Geophys. Res.: Atmosphere*, 32, L09805, doi:10.1029/2005GL022592, 2005.
- Tran, S., Bonsang, B., Gros, V., Peeken, I., Sarda-Esteve, R., Bernhardt, A., and Belviso, S.: A survey of carbon monoxide and nonmethane hydrocarbons in the Arctic Ocean during summer 2010, *Biogeosciences*, 10, 1909–1935, <https://doi.org/10.5194/bg-10-1909-2013>, 2013.
- Wang, F. W., Guo, Z. G., Lin, T., Hu, L. M., Chen, Y. J., and Zhu, Y. F.: Characterization of carbonaceous aerosols over the East China Sea: The impact of the East Asian continental outflow, *Atmos. Environ.*, 110, 163-173, 2015.